IEEE Access
Multidisciplinary : Rapid Review : Open Access Journal

Received January 19, 2021, accepted February 4, 2021, date of publication February 8, 2021, date of current version February 17, 2021.

Digital Object Identifier 10.1109/ACCESS.2021.3057923

Distributed Event-Triggered Adaptive Coordinated Trajectory Tracking Control of Multi-USVs Based on the Aggregate Tracking Error

AIHUA ZHANG, JIE ZHANG, AND LINGYAO YANG
School of Mechanical and Automotive Engineering, Shanghai University of Engineering Science, Shanghai 201620, China
Corresponding authors: Aihua Zhang (01140002@sues.edu.cn) and Jie Zhang (1246634347@qq.com)

This work was supported in part by the National Natural Science Foundation of China under Grant 51609132.

ABSTRACT Aiming to solving the nonlinear coordinated trajectory tracking control problem of multi-USVs under the influence of slowly changing and uncertain environmental disturbances, reducing energy consumption and ensuring tracking performance and stability, a distributed event-triggered adaptive coordinated trajectory tracking controller (DET-ACTTC) for multiple unmanned surface vessels (multi-USVs) is proposed based on the undirected communication topology. By introducing a virtual leader, a leader-follower formation is used to generate the coordinated tracking errors. Based on the expected formation and states, the aggregate tracking errors are defined, and event-triggered measurement errors are constructed to design the event-triggered conditions. An adaptive term is used to compensate for external environment disturbances, and the DET-ACTTC is deduced for each USV in the group. The tracking errors of the event-triggered coordinated trajectory tracking control (ETCTTC) system gradually converge to zero, and Zeno behavior is avoided. The theoretical results are verified by simulations.

INDEX TERMS Multi-USVs, coordinated trajectory tracking, event-triggered, the aggregate tracking error.

I. INTRODUCTION

A. AIMS AND MOTIVATION

As is a single unmanned surface vessel (USV) has limited operational capacity in the process of development and utilization of marine resources in a large area, multiple unmanned surface vessels (multi-USVs) coordinated operations are needed. The coordinated control method is the foundation for ensuring the efficiency, tracking accuracy and robustness of the coordinated control system; See [1]. Trajectory tracking control is the basic problem of the coordinated operation of unmanned vehicles, and coordinated trajectory tracking control has been a research hotspot in recent years; See [2]– [20].

However, in most studies, as in [2]– [10], the control instructions are updated at uniform time intervals based on the sampling time, but this can lead to unnecessary resource consumption and is often unrealistic in practical applications since continuous and frequent communication among agents has large communication costs, increased band width bearing, and increased energy consumption. To solve these problems, many significant methods have been proposed in recent years; See [11]– [34]. Due to the limited energy on board a vessel, energy-saving control systems have received increasing attention from researchers, and the event-triggered control strategy has been adopted. The control instructions are updated based on the auxiliary state and event-triggered condition; See [14]– [34].

Another problem that we need to address is determining the formation protocol in coordinated trajectory tracking control problems; See [8], [9], [14]– [17]. Among all of the formation protocols, leader-follower is used widely because it is easy to understand and implement. Considering that the control of USVs is under the influence of slowly changing and uncertain environmental disturbances, to reduce energy consumption and ensure tracking performance and stability, this paper studies adaptive event-triggered control for the coordinated trajectory tracking control system of multi-USVs based on the leader-follower formation protocol.

The associate editor coordinating the review of this manuscript and approving it for publication was Bohui Wang.

B. LITERATURE REVIEW AND BACKGROUND

Currently, the event-triggered control method has been widely studied. Aiming at a linear robot trajectory tracking system, the proportional-integral-differential (PID) control strategy with an event-triggered control strategy algorithm was adopted based on the precise model in [19]. In [20], an event-triggered control strategy for dealing with the network transmission delay was constructed. In [21], a distributed event-triggered strategy was proposed to address the consensus problem of multi agent systems. In [22] and [23], decentralized event-triggered control was studied for the multi agent consensus problem of general linear dynamics based on graph theory, and the final consensus error could only converge to a neighborhood of zero. Addressing the output consensus problem of a heterogeneous linear multi-agent system, [24] proposed a distributed event-triggered control scheme. In [25], even-triggered functions were used to solve the problem of linear multi agent consensus with augmented dynamic triggering mechanisms. On the other hand, time delay is an inevitable phenomenon in the real coordinated control systems, [35] studied the problem and proposed the robust estimation framework of synchronization error level for the multiple heterogeneous uncertain chaotic systems. And, in [26], by designing a distributed observer, the problem of event-triggered output consistency of heterogeneous multi-agent systems with time-varying communication delays is studied. Note that nearly all the controllers in the above literature are designed to address linear systems.

As a matter of fact, most practical control systems are nonlinear, and researchers have focused on nonlinear event-triggered control of multi agent systems; See [15]– [17], [27]– [34]. To achieve uniform control of first-order nonlinear systems under external disturbances, in [16], a robust distributed event-triggered control protocol was proposed based on leader-follower formations. In [17], a dynamic output feedback controller was proposed through relative measurements of neighboring agents for the consensus problem of general nonlinear multi agent systems with input saturation. In [31], according to the ratio of a certain measurement error with respect to the norm of a function of the state, a centralized event-triggered condition is designed, and centralized event-triggered formation control of multiple agents is realized. In [14], the centralized event-triggered conditions are obtained based on the measurement error and the disagreement vector.

However, designing centralized event-triggered control schemes requires knowing the global information and updating synchronously, which not only requires the transmission of more information but also lacks the flexibility to control a single agent. To further improve the utilization efficiency of communication resources, distributed event-triggered coordinated tracking control was proposed; See [15]–[18] [21]–[23], [33], [34]. For nonlinear systems, [15] proposed a distributed event-triggered model predictive control scheme, which considers the prediction state error and the convergence of the cost function, for the formation of multiple unmanned aerial vehicles. In [18], an event-triggered adaptive control scheme is developed for a class of interconnected systems, and the estimator was constructed to compensate for the influence of external disturbance and unknown measurement errors. In [16] and [33], a distributed event-triggered condition is designed based on a leader-follower formation protocol. However, a uniform lower bound for the event-triggered intervals was not provided in [33]. For uncertain nonlinear multi agent systems in the form of strict feedback, a control scheme based on fuzzy adaptive distributed event triggering is studied in [34].

Motivated by the above observations, this paper focuses on solving the nonlinear coordinated trajectory tracking control problem of multi-USVs under the influence of slowly changing and uncertain environmental disturbances, and the distributed event-triggered adaptive coordinated trajectory tracking controller (DET-ACTTC) is proposed. By combining the formation position tracking errors and speed errors of each USV, we construct an aggregate tracking error term, and the nonlinear event-triggered coordinated trajectory tracking control (ETCTTC) system is established. An adaptive term is designed to compensate for the uncertain disturbance, and the effectiveness is verified by simulations.

The main contributions of this paper are as follows:

1) Compared with the coordinated control methods in [3], [6]- [9], [35], a distributed event-triggered method is proposed, in which the control instructions are updated based on the auxiliary state and distributed event-triggered conditions, rather than updated at uniform time intervals based on the sampling time. By adopting the proposed control strategy, the energy consumption is greatly reduced.
2) In view of the fact that most piratical control system are nonlinear and with the influence of uncertain disturbances, a nonlinear event-triggered adaptive coordinated trajectory tracking control for multi-USVs is proposed, the adaptive term is designed to compensate for the uncertain disturbance, and the stability of the nonlinear event-triggered adaptive coordinated control system is obtained, unlike the linear event-triggered control methods in [21]– [26].
3) In contrast with the researches in [16], [17], [31], [33], a new event-triggered coordinated trajectory tracking control strategy for multi-USVs is presented based on the aggregated tracking errors. By using the leader-follower formation protocol and a virtual leader, the aggregated tracking errors are constructed through defining the coordinated position tracking errors and the coordinated speed tracking errors, and the stability and the trigger conditions are obtained only through building an adaptive aggregate tracking error control system, which is easier to design. Moreover, because the position tracking error is defined by using the state information of the neighboring USVs, not all vehicles need to communicate with the virtual leader, the actual communication

consumption can be greatly reduced, and it will be more energy-saving.

II. PROBLEM DESCRIPTION

Considering $N+1$ identical USVs in the multi-USVs coordinated tracking control system, assuming that the USV labeled 0 is the virtual leader, the USVs labeled are the followers. The dynamics of the *i-th* USV are described as [2]

$$\begin{aligned} \boldsymbol{M}_i\dot{\boldsymbol{\nu}}_i &= -\boldsymbol{C}_i\boldsymbol{\nu}_i - \boldsymbol{D}_i(\boldsymbol{\nu}_i) + \boldsymbol{\tau}_i + \boldsymbol{d}_i \\ \dot{\boldsymbol{\eta}}_i &= \boldsymbol{J}(\psi_i)\boldsymbol{\nu}_i \end{aligned} \tag{1}$$

where $\boldsymbol{\eta}_i = (x_i, y_i, \psi_i)^T \in \Re^3$ denotes the position of follower USV in an earth-fixed frame, x_i is the northbound position, y_i is the eastbound position, and ψ_i is the yaw angle. $\boldsymbol{\nu}_i = (u_i, v_i, r_i)^T \in \Re^3$ denotes the velocity in the body-fixed frame, u_i is the speed in surge, v_i is the speed in sway and r_i is the angle speed in the yaw directions. $\boldsymbol{J}(\psi_i)$ denotes the transformation matrix from the earth-fixed frame to the body-fixed frame, as shown in (2). Matrix $\boldsymbol{M}_i(\boldsymbol{\nu}_i)$ is the inertia parameter matrix, which satisfies $\boldsymbol{M}_i(\boldsymbol{\nu}_i) > 0$. Matrix $\boldsymbol{C}_i(\boldsymbol{\nu}_i)$ is the Coriolis and centripetal matrix and matrix $\boldsymbol{D}_i$ represents a damping matrix. $\boldsymbol{\tau}_i$ is the control input, and d_i denotes the uncertain external environment disturbances.

$$\boldsymbol{J}(\psi_i) = \begin{bmatrix} \cos\psi_i & -\sin\psi_i & 0 \\ \sin\psi_i & \cos\psi_i & 0 \\ 0 & 0 & 1 \end{bmatrix} \tag{2}$$

In this paper, we consider all USVs use the same hardware configuration, the communication graph among the $N+1$ USVs can be represented by an undirected graph Ξ, which satisfies the following assumption.

Assumption 1: The communication graph among multi-USVs is undirected and connected.

Assumption 2: The reference trajectory $\boldsymbol{\eta}_d$ is smooth and differentiable. For any time $t > t_0$, there are normal numbers c_1, c_2 that make the reference trajectory $\boldsymbol{\eta}_d$ satisfy $\|\dot{\boldsymbol{\eta}}_d(t)\| \leq c_1, \|\ddot{\boldsymbol{\eta}}_d(t)\| \leq c_2$.

III. THE LEADER-FOLLOWING FORMATION METHOD WITH A VIRTUAL LEADER

Assume there is a virtual leader in coordination tracking, only the leader knows the global information of the task and the followers keep fixed relative attitudes and distances from the leader. Assume there are N USVs, the $0-th$ USV is introduced as the virtual leader, and the expected relative position is defined as $\boldsymbol{l}_i = [x_i, y_i, \psi_i]$, $i = 1, \cdots, N$, between each follower and virtual leader 0. The position relation diagram of the multi-USVs coordinated formation method is shown in Fig.1.

Based on the state information of the neighboring USVs, the position tracking error $\tilde{\boldsymbol{\eta}}_i$ of the *i-th* USV is defined as

$$\tilde{\boldsymbol{\eta}}_i = \sum_{j=0}^{N} a_{ij}(\boldsymbol{J}(\psi_i)^T\boldsymbol{\eta}_i - (\boldsymbol{J}(\psi_j)^T\boldsymbol{\eta}_j - l_j) - l_i) \tag{3}$$

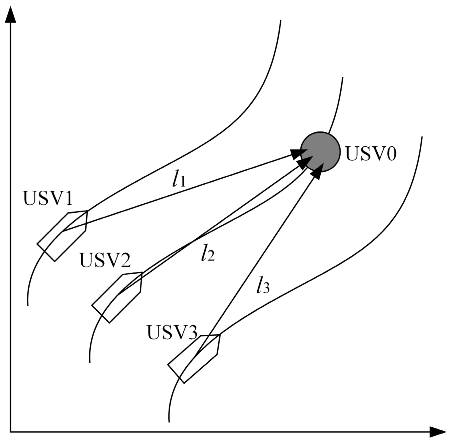

FIGURE 1. The related positions of USVs.

Then, the speed tracking error $\tilde{\boldsymbol{\nu}}_i$ is defined as

$$\tilde{\boldsymbol{\nu}}_i = \sum_{j=0}^{N} a_{ij}(\boldsymbol{\nu}_i - \boldsymbol{\nu}_j) \tag{4}$$

where a_{ij} is the (i, j) term of the adjacency matrix $\boldsymbol{L}$ related to graph Ξ, $a_{ij} > 0$ indicates that information about the *i-th* USV can be passed to the *j-th* USV, and otherwise $a_{ij} = 0$.

IV. DISTRIBUTED EVENT-TRIGGERED ADAPTIVE COORDINATED TRAJECTORY TRACKING CONTROL

With (3) and (4), the model of the coordinated tracking control system of multi–USVs is obtained

$$\begin{cases} \boldsymbol{M}_i\dot{\tilde{\boldsymbol{\nu}}}_i = & \sum_{j=0}^{N} a_{ij}(-\boldsymbol{C}_i\boldsymbol{\nu}_i - \boldsymbol{D}_i\boldsymbol{\nu}_i + \boldsymbol{\tau}_i) + \boldsymbol{d}_i{}' \\ & -\boldsymbol{M}_i\sum_{j=0}^{N} a_{ij}\boldsymbol{M}_j^{-1}(-\boldsymbol{C}_j\boldsymbol{\nu}_j - \boldsymbol{D}_j\boldsymbol{\nu}_j + \boldsymbol{\tau}_j) \\ \dot{\tilde{\boldsymbol{\eta}}}_i = & \sum_{j=0}^{N} a_{ij}(\dot{\boldsymbol{J}}(\psi_i)^T\boldsymbol{\eta}_i + \boldsymbol{J}(\psi_i)^T\dot{\boldsymbol{\eta}}_i) \\ & -(\dot{\boldsymbol{J}}(\psi_j)^T\boldsymbol{\eta}_j + \boldsymbol{J}(\psi_j)^T\dot{\boldsymbol{\eta}}_j) \end{cases} \tag{5}$$

where

$$\boldsymbol{d}_i{}' = \sum_{j=0}^{N} a_{ij}\boldsymbol{d}_i - \boldsymbol{M}_i\sum_{j=0}^{N} a_{ij}\boldsymbol{M}_j^{-1}\boldsymbol{d}_j \tag{6}$$

$$\dot{\boldsymbol{J}}(\psi_i)^T\boldsymbol{\eta}_i = (\boldsymbol{J}(\psi_i)\boldsymbol{S})'(\boldsymbol{H}\boldsymbol{J}(\psi_i)\boldsymbol{\nu}_i\boldsymbol{\eta}_i) + \boldsymbol{J}(\psi_i)'\boldsymbol{J}(\psi_i)\boldsymbol{\nu}_i \tag{7}$$

$$\boldsymbol{S} = \begin{bmatrix} 0 & -1 & 0 \\ 1 & 0 & 0 \\ 0 & 0 & 0 \end{bmatrix} \tag{8}$$

$$\boldsymbol{H} = \begin{bmatrix} 0 & 0 & 1 \end{bmatrix} \tag{9}$$

$\boldsymbol{\xi}_i$ is defined as the aggregate tracking error of the *i-th* USV

$$\boldsymbol{\xi}_i = \tilde{\boldsymbol{\nu}}_i + \boldsymbol{B}_i\tilde{\boldsymbol{\eta}}_i \tag{10}$$

where $\boldsymbol{B}_i \in \Re^{3\times 3}$ is a positive definite matrix.

Remark 1: The convergence of $\boldsymbol{\xi}_i$ can guarantee the convergence of $\tilde{\boldsymbol{\nu}}_i$ and $\tilde{\boldsymbol{\eta}}_i$ (See [10]).

Assumption 3: The leader's control input $\boldsymbol{\tau}_0$ is bounded; i.e., $\|\boldsymbol{\tau}_0\| \leq \gamma$, where $\gamma > 0$ and the external disturbances $\boldsymbol{d}_i$ of the *i-th* USV is bounded, and $\|\boldsymbol{d}_i\| \leq d$, where $d > 0$.

It is known that if the control input $\boldsymbol{\tau}_i, i = 1, \cdots, N$ of (1) could make $\lim_{t\to\infty} \tilde{\boldsymbol{\eta}}_i = 0$, $\lim_{t\to\infty} \tilde{\boldsymbol{\nu}}_i = 0$, for $i = 1, \cdots, N$; hence, the coordinated trajectory tracking problem is solved.

Therefore, based on the local information of the neighboring USVs, the DET-ACTTC is given as

$$\begin{cases} \boldsymbol{\tau}_i = & (\boldsymbol{M}_i\dot{\boldsymbol{\nu}}_i + \boldsymbol{C}_i\boldsymbol{\nu}_i) - (\boldsymbol{M}_i\dot{\tilde{\boldsymbol{\nu}}}_i + \boldsymbol{C}_i\tilde{\boldsymbol{\nu}}_i) \\ & -(\boldsymbol{M}_i\dot{\tilde{\boldsymbol{\eta}}}_i + \boldsymbol{C}_i\boldsymbol{B}_i\tilde{\boldsymbol{\eta}}_i) + \boldsymbol{D}_i\boldsymbol{\nu}_i - \hat{\boldsymbol{d}}_i \\ & -\sum_{j=1}^{N} a_{ij}\left[\boldsymbol{\xi}_i(t_{ki}^i) - \boldsymbol{\xi}_j(t_{kj}^j)\right] \\ \dot{\hat{\boldsymbol{d}}}_i = & \boldsymbol{\kappa}_i\boldsymbol{\xi}_i \end{cases} \tag{11}$$

where $\boldsymbol{\xi}_i$ is defined as in (11), $\hat{\boldsymbol{d}}_i$ is the estimation of the uncertain external environment disturbances, and $\boldsymbol{\kappa}_i$ are positive numbers. $\boldsymbol{\xi}_i(t_{k_i}^i)$ is the aggregate tracking error of the *i-th* USV's last triggered event. $t_{k_i}^i, k_i = 1, 2, \cdots$ is the moment when the last event of the *i-th* USV is triggered.

For the *i-th* USV, we define the event-triggered measurement error as

$$\boldsymbol{e}_i = \boldsymbol{\xi}_i(t_{ki}^i) - \boldsymbol{\xi}_i(t), t \geq 0 \tag{12}$$

And the event-triggered condition is designed as

$$f_i(t, \boldsymbol{e}_i(t)) = \|\boldsymbol{e}_i(t)\| - T_i(\boldsymbol{\xi}_i(t_{ki}^i)) \tag{13}$$

where

$$T_i(\boldsymbol{\xi}_i(t_{ki}^i)) = \frac{\lambda_i(\frac{1}{2}\sum_{j=1}^{N} a_{ij}\left\|\boldsymbol{\xi}_i(t_{ki}^i) - \boldsymbol{\xi}_j(t_{kj}^j)\right\|^2)}{\left\|\sum_{j=1}^{N} a_{ij}(\boldsymbol{\xi}_i(t_{ki}^i) - \boldsymbol{\xi}_j(t_{kj}^j))\right\|} > 0 \tag{14}$$

and $0 < \lambda_i < 1$ is a parameter to be determined. When the event-triggered measurement error of the *i-th* USV is greater than its threshold, which means $f_i(t, e_i(t)) = \|\boldsymbol{e}_i(t) = T_i(\boldsymbol{\xi}_i(t_{k_i}^i))\|$, the control scheme of the *i-th* USV is updated. Then, the *i-th* USV broadcasts its current state to its neighboring USVs. At the same time, the measurement error of the *i-th* USV is reset to zero. When the *i-th* USV receives a new state from another neighboring USV, the USV also immediately updates the controller. In the process of state measurement, if and only if the position tracking error of the multi-USVs system is 0, that is $\boldsymbol{\xi}_i = \boldsymbol{0}$, $i = 1, \cdots, N$, the threshold denominator of the event-triggered measurement error $\|\sum_{j=1}^{N} a_{ij}(\boldsymbol{\xi}_i(t_{k_i}^i) - \boldsymbol{\xi}_j(t_{k_j}^j))\| = 0$; then, instead of judging whether the event-triggered conditions are satisfied, the controller is driven directly by the control instruction at the last triggered time.

By substituting (11) into (5), the closed-loop system equation is rewritten as

$$\boldsymbol{M}_i\dot{\boldsymbol{\xi}}_i + \boldsymbol{C}_i\boldsymbol{\xi}_i = -\sum_{j=1}^{N} a_{ij}(\boldsymbol{\xi}_i(t_{ki}^i) - \boldsymbol{\xi}_j(t_{kj}^j)) - \hat{\boldsymbol{d}}_i + \boldsymbol{d}_i \tag{15}$$

The Lyapunov function is chosen as

$$V = \frac{1}{2}\sum_{i=1}^{N} \boldsymbol{\xi}_i^T\boldsymbol{M}_i\boldsymbol{\xi}_i + \frac{1}{2}\sum_{i=1}^{N} \tilde{\boldsymbol{d}}_i^T\kappa_i^{-1}\tilde{\boldsymbol{d}}_i \tag{16}$$

where $\boldsymbol{M}_i(\boldsymbol{\nu}_i) > 0$, $\boldsymbol{\kappa}_i > 0$ and $\tilde{\boldsymbol{d}}_i = \hat{\boldsymbol{d}}_i - \boldsymbol{d}_i$ is the estimation error of the slowly changing and uncertain environmental disturbances; then, $\dot{\boldsymbol{d}}_i = 0$.

Substituting (11) and (15) into (16), the time derivative of V along $\boldsymbol{d}_i$ and $\boldsymbol{\xi}_i$ is

$$\begin{aligned} \dot{V} &= \frac{1}{2}\sum_{i=1}^{N} \boldsymbol{\xi}_i^T\dot{\boldsymbol{M}}_i\boldsymbol{\xi}_i + \sum_{i=1}^{N} \boldsymbol{\xi}_i^T\boldsymbol{M}_i\dot{\boldsymbol{\xi}}_i + \sum_{i=1}^{N} \tilde{\boldsymbol{d}}_i\boldsymbol{\kappa}_i^{-1}\dot{\tilde{\boldsymbol{d}}}_i \\ &= \frac{1}{2}\sum_{i=1}^{N} \boldsymbol{\xi}_i^T\dot{\boldsymbol{M}}_i\boldsymbol{\xi}_i + \sum_{i=1}^{N} \boldsymbol{\xi}_i^T\boldsymbol{M}_i\dot{\boldsymbol{\xi}}_i + \sum_{i=1}^{N} \tilde{\boldsymbol{d}}_i\boldsymbol{\kappa}_i^{-1}(\dot{\hat{\boldsymbol{d}}}_i - \dot{\boldsymbol{d}}_i) \\ &= \frac{1}{2}\sum_{i=1}^{N} \boldsymbol{\xi}_i^T\dot{\boldsymbol{M}}_i\boldsymbol{\xi}_i + \sum_{i=1}^{N} \boldsymbol{\xi}_i^T(-\sum_{j=1}^{N} a_{ij}(\boldsymbol{\xi}_i(t_{ki}^i) - \boldsymbol{\xi}_j(t_{kj}^j)) \\ &\quad -\hat{\boldsymbol{d}}_i + \boldsymbol{d}_i - \boldsymbol{C}_i\boldsymbol{\xi}_i) + \sum_{i=1}^{N} \tilde{\boldsymbol{d}}_i\boldsymbol{\kappa}_i^{-1}(\dot{\hat{\boldsymbol{d}}}_i - \dot{\boldsymbol{d}}_i) \\ &= \sum_{i=1}^{N} \boldsymbol{\xi}_i^T(\frac{1}{2}\dot{\boldsymbol{M}}_i - \boldsymbol{C}_i)\boldsymbol{\xi}_i - \sum_{i=1}^{N} \boldsymbol{\xi}_i^T\tilde{\boldsymbol{d}}_i + \sum_{i=1}^{N} \tilde{\boldsymbol{d}}_i\boldsymbol{\xi}_i \\ &\quad -\sum_{i=1}^{N} \boldsymbol{\xi}_i^T\sum_{j=1}^{N} a_{ij}(\boldsymbol{\xi}_i(t_{ki}^i) - \boldsymbol{\xi}_j(t_{kj}^j)) \\ &= \sum_{i=1}^{N} \boldsymbol{\xi}_i^T(\frac{1}{2}\dot{\boldsymbol{M}}_i - \boldsymbol{C}_i)\boldsymbol{\xi}_i \\ &\quad -\sum_{i=1}^{N} \boldsymbol{\xi}_i^T\sum_{j=1}^{N} a_{ij}(\boldsymbol{\xi}_i(t_{ki}^i) - \boldsymbol{\xi}_j(t_{kj}^j)) \end{aligned} \tag{17}$$

Because of the antisymmetric property of the Lagrangian system, $\frac{1}{2}\dot{\boldsymbol{M}}_i = \boldsymbol{C}_i$. Therefore, equation (17) can be simplified as

$$\begin{aligned} \dot{V} &= -\sum_{i=1}^{N} \boldsymbol{\xi}_i^T\sum_{j=1}^{N} a_{ij}(\boldsymbol{\xi}_i(t_{ki}^i) - \boldsymbol{\xi}_j(t_{kj}^j)) \\ &= -\sum_{i=1}^{N} (\boldsymbol{\xi}_i(t_{ki}^i) - \boldsymbol{e}_i)^T\sum_{j=1}^{N} a_{ij}(\boldsymbol{\xi}_i(t_{ki}^i) - \boldsymbol{\xi}_j(t_{kj}^j)) \\ &= -\sum_{i=1}^{N} \boldsymbol{\xi}_i(t_{ki}^i)^T\sum_{j=1}^{N} a_{ij}(\boldsymbol{\xi}_i(t_{ki}^i) - \boldsymbol{\xi}_j(t_{kj}^j)) \\ &\quad +\sum_{i=1}^{N} \boldsymbol{e}_i^T\sum_{j=1}^{N} a_{ij}(\boldsymbol{\xi}_i(t_{ki}^i) - \boldsymbol{\xi}_j(t_{kj}^j)) \end{aligned} \tag{18}$$

Since the undirected communication graph is balanced, the in-degree and the out-degree are equal for all nodes, which means $\sum_{j=1}^{N} a_{ij} = \sum_{i=1}^{N} a_{ji}$; then, we have

$$
\begin{aligned}
&-\sum_{i=1}^{N}\boldsymbol{\xi}_i(t_{ki}^i)^T\sum_{j=1}^{N}a_{ij}(\boldsymbol{\xi}_i(t_{ki}^i)-\boldsymbol{\xi}_j(t_{kj}^j))\\
&=-\sum_{i=1}^{N}\sum_{j=1}^{N}a_{ij}(\left\|\boldsymbol{\xi}_i(t_{ki}^i)\right\|^2-\boldsymbol{\xi}_i^T(t_{ki}^i)\boldsymbol{\xi}_j(t_{kj}^j))\\
&=-\sum_{i=1}^{N}\sum_{j=1}^{N}a_{ij}(\frac{\left\|\boldsymbol{\xi}_i(t_{ki}^i)\right\|^2}{2}+\frac{\left\|\boldsymbol{\xi}_j(t_{kj}^j)\right\|^2}{2}-\boldsymbol{\xi}_i^T(t_{ki}^i)\boldsymbol{\xi}_j(t_{kj}^j))\\
&\leq-\frac{1}{2}\sum_{i=1}^{N}\sum_{j=1}^{N}a_{ij}\left\|\boldsymbol{\xi}_i(t_{ki}^i)-\boldsymbol{\xi}_j(t_{kj}^j)\right\|^2 \qquad (19)
\end{aligned}
$$

Obviously, the following inequality holds

$$
\begin{aligned}
&\sum_{i=1}^{N}\boldsymbol{e}_i^T\sum_{j=1}^{N}a_{ij}(\boldsymbol{\xi}_i(t_{ki}^i)-\boldsymbol{\xi}_j(t_{kj}^j))\\
&\leq\sum_{i=1}^{N}\|\boldsymbol{e}_i\|\left\|\sum_{j=1}^{N}a_{ij}(\boldsymbol{\xi}_i(t_{ki}^i)-\boldsymbol{\xi}_j(t_{kj}^j))\right\| \qquad (20)
\end{aligned}
$$

Then, we have

$$
\begin{aligned}
\dot{V}\leq&-\frac{1}{2}\sum_{i=1}^{N}\sum_{j=1}^{N}a_{ij}\left\|\boldsymbol{\xi}_i(t_{ki}^i)-\boldsymbol{\xi}_j(t_{kj}^j)\right\|^2\\
&+\sum_{i=1}^{N}\|\boldsymbol{e}_i\|\left\|\sum_{j=1}^{N}a_{ij}(\boldsymbol{\xi}_i(t_{ki}^i)-\boldsymbol{\xi}_j(t_{kj}^j))\right\| \qquad (21)
\end{aligned}
$$

Because the event-triggered condition $f_i(t,\boldsymbol{e}_i(t)) \leq 0$ is satisfied for each USV before the next event-triggered time occurs, then

$$
\dot{V}\leq\frac{1}{2}(\lambda_i-1)(\sum_{i=1}^{N}\sum_{j=1}^{N}a_{ij}\left\|\boldsymbol{\xi}_i(t_{ki}^i)-\boldsymbol{\xi}_j(t_{kj}^j)\right\|^2)\leq 0 \qquad (22)
$$

On the basis of the stability theory of Lyapunov, we have $\lim_{t\to\infty}\boldsymbol{\xi}_i \to 0$, $\lim_{t\to\infty}\tilde{\boldsymbol{d}}_i \to 0$ according (16). According to the Remark 1, we have $\lim_{t\to\infty}\tilde{\boldsymbol{\eta}}_i \to 0$, $\lim_{t\to\infty}\tilde{\boldsymbol{\nu}}_i \to 0$. Hence, we can obtain the following theorem.

Theorem 1: Suppose that Assumption 1, Assumption 2, and Assumption 3 hold; for system (5), the DET-ACTTC can make the aggregate tracking errors described in (10), the position tracking errors and the speed tracking errors of each USV converge to zero gradually.

V. ELIMINATION OF ZENO PHENOMENON

Assume the controller of the *i-th* USV is triggered at time k_i, and let $t = t^*$. According to the definition of the state-based measurement error in (12), we know that $\dot{\boldsymbol{e}}_i = -\dot{\boldsymbol{\xi}}_i(t)$ holds for $t \in (t_{k_i}^i, t_{k_{i+1}}^i)$, where $\boldsymbol{\xi}_i(t)$ is bounded.

Because of the boundedness property of the Lagrangian system, we know that $\boldsymbol{M}_i(\boldsymbol{\nu}_i)$ and $\boldsymbol{C}_i(\boldsymbol{\nu}_i)$ are bounded. It is obvious that $\dot{\boldsymbol{\xi}}_i(t)$ is also bounded according to (17). Therefore, $\|\dot{\boldsymbol{e}}_i(t)\| = \|\dot{\boldsymbol{\xi}}_i(t)\|$ has upper bound N for $t \in (t_{k_i}^i, t_{k_{i+1}}^i)$.

In addition, because the event-triggered measurement errors were set to zero when the *i-th* USV was triggered, i.e., $\boldsymbol{e}_i(t^*) = \boldsymbol{0}_p$, the following formula $\|\boldsymbol{e}_i(t)\| = \left\|\int_{t^*}^{t}\dot{\boldsymbol{e}}_i(s)ds + \boldsymbol{e}_i(t^*)\right\| \leq \int_{t^*}^{t}\|\dot{\boldsymbol{e}}_i(s)\|\,ds = (t-t^*)N$ is established in [10]; hence, $(t-t^*) \geq \|\boldsymbol{e}_i(t)\|/N \geq 0$. Notably, when $\|\boldsymbol{e}_i(t)\| = 0$ the event-triggered conditions in (13) are not met; hence, the event-triggered controller does not act on the multi-USVs system. Then, each time interval between two events must be greater than zero. Therefore, for the *i-th* USV, the trigger interval of the control input is always greater than zero; i.e., $(t-t^*) > 0$, which means that the Zeno phenomenon does not occur in the system.

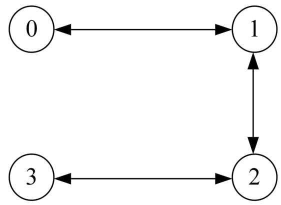

FIGURE 2. Communication topology between followers and virtual leader.

VI. SELECTION OF CONTROL PARAMETERS

Now, we have designed the DET-ACTTC for a multi-USVs system and proved the stability of the closed-loop control system in the sense of Lyapunov. However, whether the proposed control scheme can achieve satisfactory trajectory tracking performance while maintaining the expected formation depends on the selection of the control parameters.

Selection of $\boldsymbol{B}_i$: From (10), we can see that the parameter $\boldsymbol{B}_i > \boldsymbol{0}$ mainly determines the trajectory tracking error of the USV. First, we adjusted $B_{i(33)}$ over a wide range, and finally, we set $B_{1(33)} = 2, B_{2(33)} = 4, B_{3(33)} = 5$. Second, according to the small range deviation in the north position and the east position during the process of trajectory tracking, $B_{i(11)}$ and $B_{i(22)}$ are adjusted, respectively, and finally, we set $B_{1(11)} = 0.015, B_{2(11)} = 0.01, B_{3(11)} = 0.01$ and $B_{1(22)} = 0.01, B_{2(22)} = 0.02, B_{3(22)} = 0.1$.

Selection of λ_i: From (14), it can be seen that the parameter $0 < \lambda_i < 1$ determines the number of triggering times of the USV. Selecting a smaller value for λ_i results in a reduction in the event-triggered times, which decrease trajectory tracking accuracy. Considering the trade-off between trajectory tracking accuracy and fewer event-trigger times, we set $\lambda_1 = 0.2, \lambda_2 = 0.5, \lambda_3 = 0.1$.

Selection of $\boldsymbol{\kappa}_i$: In this paper, the adaptive term in (11) is used to compensate for the external environment disturbances, so the parameters $\boldsymbol{\kappa}_i > \boldsymbol{0}$ directly affect the magnitude of the system chattering. By continuous adjustments and comparative analysis, we set $\kappa_{i_1} = 0.01, \kappa_{i_2} = 0.01, \kappa_{i_3} = 0.01$.

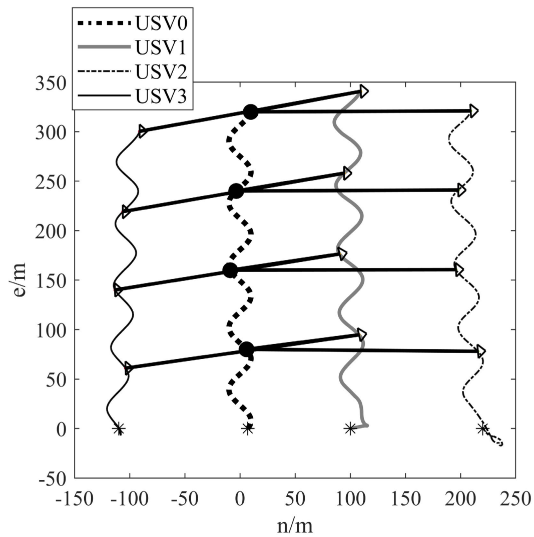

FIGURE 3. The curves of USV trajectory tracking variations.

VII. SIMULATION EXAMPLES

In this section, a numerical simulation example is carried out to show the effectiveness of the proposed DET-ACTTC. The coordination operations are achieved by three USVs. The communication topology of the event-triggered coordination control system is shown in Fig.2, in which the USV labeled 0 is the virtual leader and the USVs labeled 1 to 3 are the followers.

The Laplacian matrix of the communication topology is

$$\boldsymbol{L} = \begin{bmatrix} 1 & -1 & 0 & 0 \\ -1 & 2 & -1 & 0 \\ 0 & -1 & 2 & -1 \\ 0 & 0 & -1 & 1 \end{bmatrix}$$

The parameters of the USVs are chosen as

$$\boldsymbol{M} = \begin{bmatrix} 25.8 & 0 & 0 \\ 0 & 33.8 & 1.0115 \\ 0 & 1.0115 & 2.76 \end{bmatrix}$$

$$\boldsymbol{C} = \begin{bmatrix} 0 & 0 & -M_{2.2}v - M_{2.3}r \\ 0 & 0 & M_{1.1}u \\ M_{2.2}v + M_{2.3}r & -M_{1.1}u & 0 \end{bmatrix}$$

$$\boldsymbol{D} = \begin{bmatrix} 0.72 + 1.33u & 0 & 0 \\ 0 & 0.86 + 36.28\,|v| & -0.11 \\ 0 & -0.11 - 5.04\,|v| & 0.5 \end{bmatrix}$$

The initial positions of the three USVs are $\boldsymbol{\eta}_1 = \begin{bmatrix} 100 & 0 & 0 \end{bmatrix}^T$, $\boldsymbol{\eta}_2 = \begin{bmatrix} 220 & 0 & 0 \end{bmatrix}^T$, $\boldsymbol{\eta}_3 = \begin{bmatrix} -110 & 0 & 0 \end{bmatrix}^T$. The disturbance terms are $\boldsymbol{d}_1 = [20\,,20\,,0]^T, \boldsymbol{d}_2 = [30\,,30\,,0]^T$ and $\boldsymbol{d}_3 = [40\,,40\,,0]^T$. The parameters related to the formation are set as $\boldsymbol{l}_0 = \begin{bmatrix} 0\,0\,0 \end{bmatrix}^T$, $\boldsymbol{l}_1 = \begin{bmatrix} 100 & 20 & 0 \end{bmatrix}^T, \boldsymbol{l}_2 = \begin{bmatrix} 200 & 0 & 0 \end{bmatrix}^T, l_3 = \begin{bmatrix} -100 & -20 & 0 \end{bmatrix}^T$.

The simulation results are shown in Fig. 3- Fig. 9.

Fig.3 shows the trajectory tracking variation curves. We can see that the USV group completes the coordinated tracking task and maintains the predetermined formation during tracking. Fig.4 shows the position and speed tracking curves in different directions. All USVs arrive at the desired position and heading angle quickly and keep up with each other. Fig.5 shows the change in tracking errors during tracking. From this figure, we can see that all of the tracking state errors eventually tend to zero.

Fig.6 shows the curves of the aggregate tracking errors. The aggregate tracking error of each USV oscillates at the

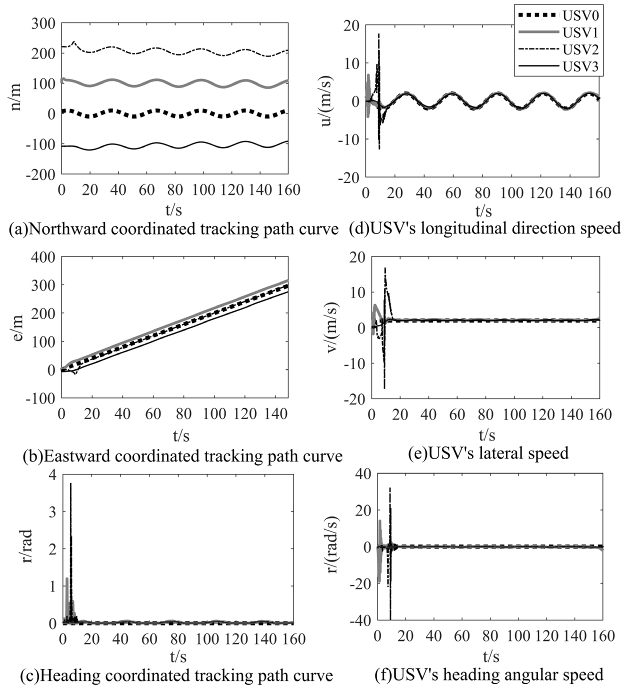

FIGURE 4. Curves of USV positions and speed tracking.

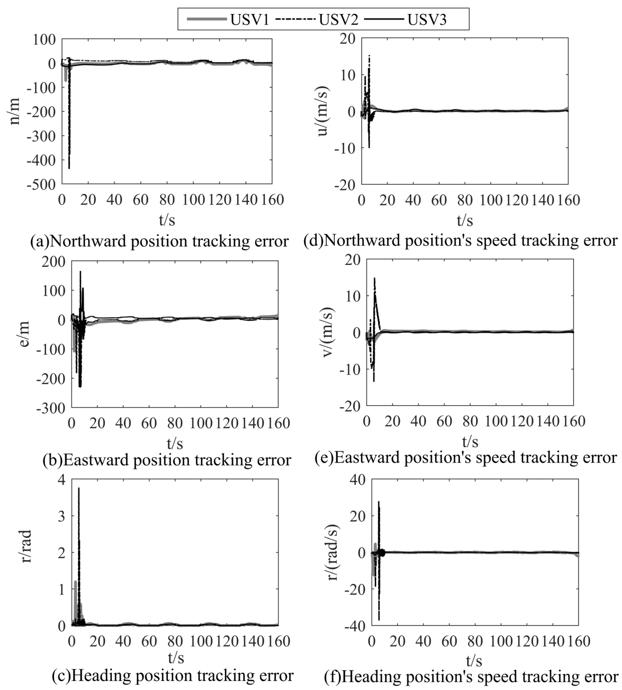

FIGURE 5. Curves of USV tracking errors and speed tracking errors.

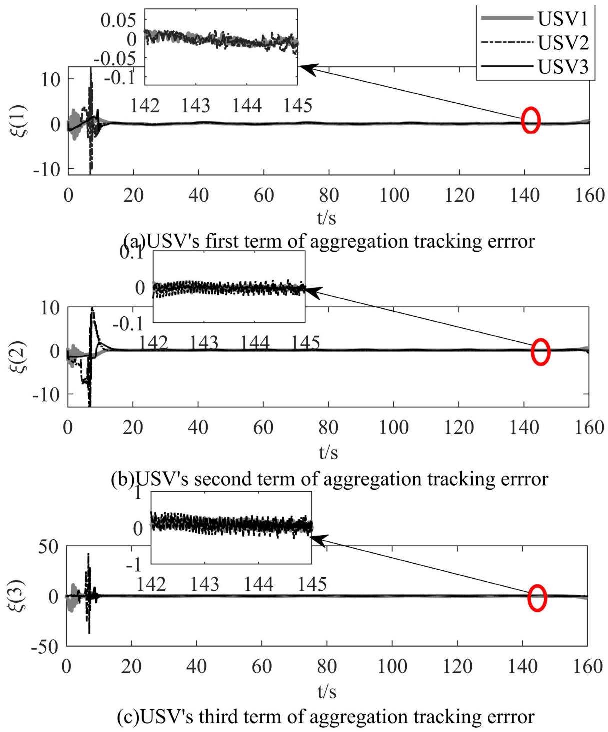

FIGURE 6. The curves of the aggregate tracking errors.

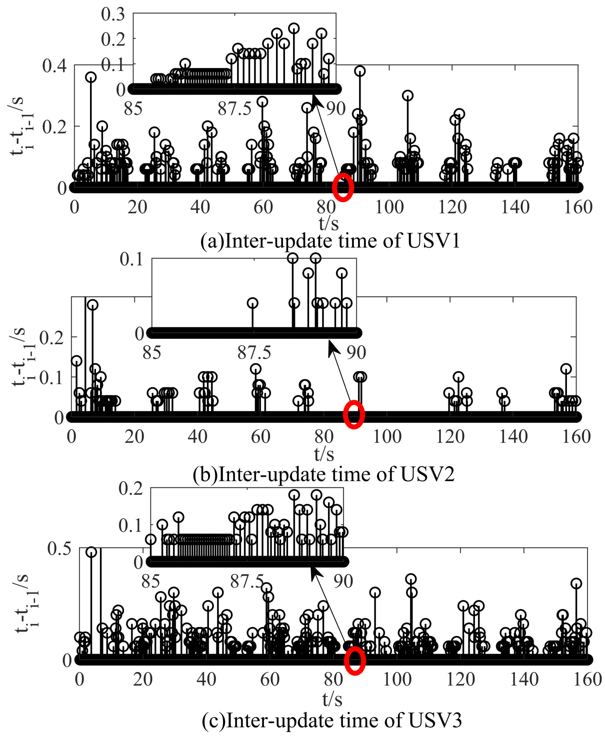

FIGURE 7. Interupdate time of the follower USV and its event-triggered measurement errors and threshold.

beginning and they converge to zero rapidly. The variation figures of each follower's interupdate time, event-triggered measurement error $\|\boldsymbol{e}_i(t)\|$ and threshold $T_i(\boldsymbol{\xi}_i(t^i_{ki}))$ are given in Fig.7 and Fig.8. Interval sampling is carried out, and Fig.7 more clearly displays the event-triggered effect. Clearly, the variation in the interupdate time is related to $\|\boldsymbol{e}_i(t)\|$ and $T_i(\boldsymbol{\xi}_i(t^i_{ki}))$, which means it is related to the aggregate tracking errors shown in Fig. 6.The reason why the interupdate time is longer in the first 10 seconds is that $T_i(\boldsymbol{\xi}_i(t^i_{ki}))$ is larger than $\|\boldsymbol{e}_i(t)\|$; the event-triggered conditions $f_i(t, \boldsymbol{e}_i(t)) > 0$ are not met for a longer time. Fig.7 shows that the minimum value of the adjacent event-triggered interval is greater than 0, which means that event-triggered control is feasible. Fig.7 shows that the interupdate time of USV 2 is mostly very short; that is, the event is triggered more times. Most of the interupdates of USV 1 and USV 3 are greater than 10 times the minimum sampling time, and there are fewer event triggering times, which also verifies the event trigger time in Fig.10. Since USV 2 communicates with USV 1 and USV 3, the event triggering of USV 1 and USV 3 may also cause the event triggering of USV 2 according to the analysis of (11). Therefore, the USV 2 event is triggered more frequently.

Fig.9 shows the change in the control instructions of each USV. It can be seen that the control instructions are segmented, which indicates that the event-triggered controllers are updated only when the event-triggered conditions are met. Fig.10 shows the histogram of the event-triggered times of the three USVs. From Fig.10, it can be seen that the update times of the three USV followers are 4235, 6079 and 3199, and they

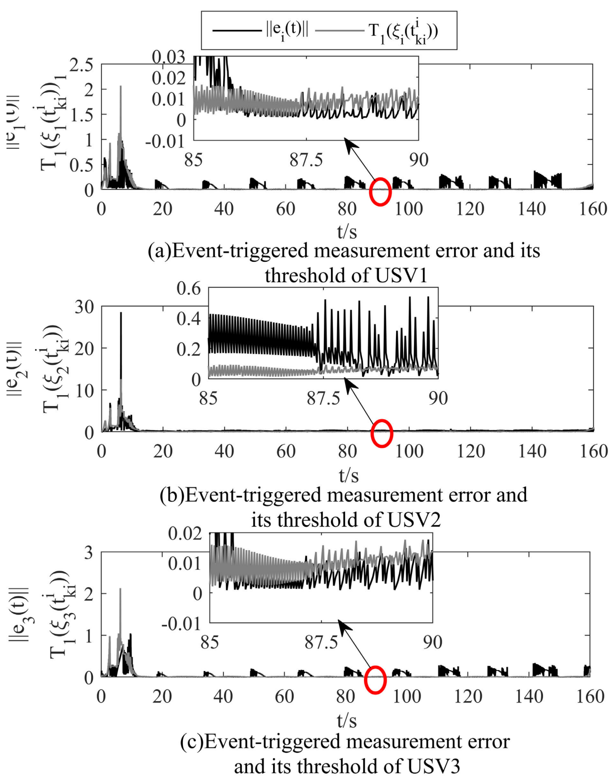

FIGURE 8. The follower USV's event-triggered measurement errors and threshold.

are greatly reduced compared with the update times of traditional uniform time intervals control method, which are all

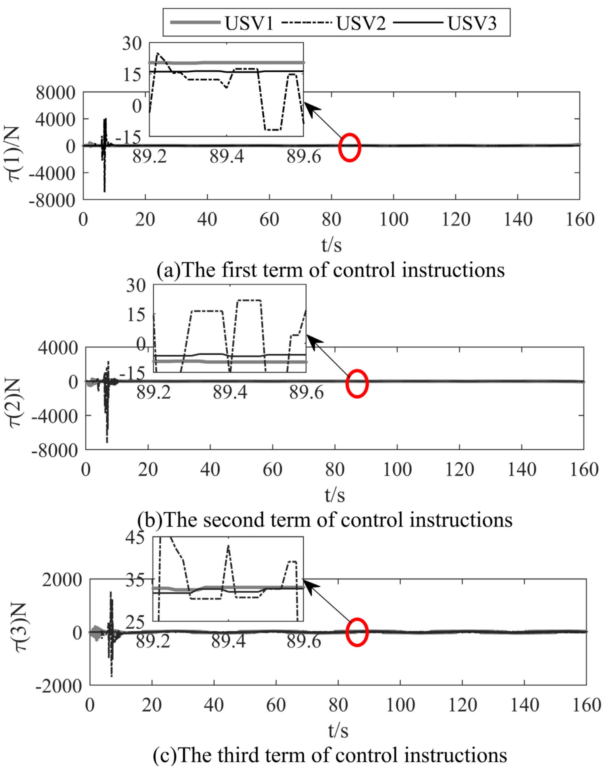

FIGURE 9. The curves of the control torque of the follower USV.

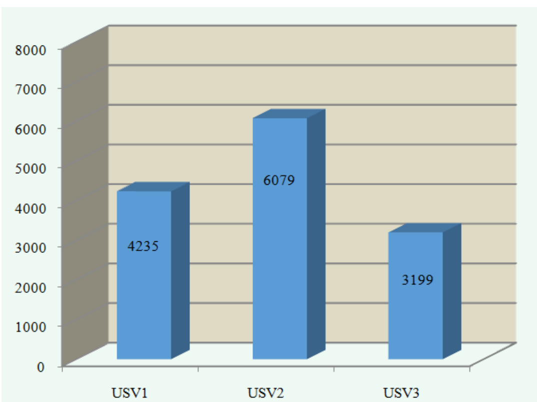

FIGURE 10. The triggered times of the follower USVs.

8000 times. Therefore, the proposed DET-ACTTC can reduce energy consumption and improve system life. The reason why the trigger times of USV 2 are significantly greater than those of the other two is that its distributed event-triggered conditions are influenced by USV 1 and USV 3 according to the communication topology shown in Fig.2 and (13).

VIII. CONCLUSION

This paper proposes the DET-ACTTC to reduce the energy consumption of the coordinated trajectory tracking control system of multi-USVs and to guarantee tracking performance and stability. Based on the aggregation tracking error, the event-triggered coordinated control equations for multi-USVs coordinated tracking are constructed, an adaptive term is designed to compensate for the disturbance on each USV, and the control instruction is updated only when the proposed event-triggered conditions are met. Lyapunov stability theory is used to prove that the tracking errors converge to zero. The simulation results show the control effect on coordinated trajectory tracking and saving communication resources. However, communication delay is an inevitable problem in the communication process. Applying a combined measurement method to achieve event triggering at only the trigger time and solving the coordinated trajectory tracking problem of multiple USVs with communication delays are the directions of our future research.

ACKNOWLEDGMENT

The authors would like to express their sincere thanks to the reviewers for their valuable suggestions and comments.

REFERENCES

[1] R. M. Murray, "Recent research in cooperative control of multivehicle systems," *J. Dyn. Syst., Meas., Control*, vol. 129, no. 5, pp. 571–583, Sep. 2007.
[2] T. I. Fossen, *Handbook of Marine Craft Hydrodynamics and Motion Control*. New York, NY, USA: Wiley, 2011.
[3] X. Liang, X. Qu, Y. Hou, Y. Li, and R. Zhang, "Distributed coordinated tracking control of multiple unmanned surface vehicles under complex marine environments," *Ocean Eng.*, vol. 205, Jun. 2020, Art. no. 107328.
[4] Z.-Q. Liu, Y.-L. Wang, and T.-B. Wang, "Incremental predictive control-based output consensus of networked unmanned surface vehicle formation systems," *Inf. Sci.*, vols. 457–458, pp. 166–181, Aug. 2018.
[5] B. S. Park and S. J. Yoo, "Adaptive-observer-based formation tracking of networked uncertain underactuated surface vessels with connectivity preservation and collision avoidance," *J. Franklin Inst.*, vol. 356, no. 15, pp. 7947–7966, Oct. 2019.
[6] L. Sorbi, G. P. D. Capua, J.-G. Fontaine, and L. Toni, "A behavior-based mission planner for cooperative autonomous underwater vehicles," *Mar. Technol. Soc. J.*, vol. 46, no. 2, pp. 32–44, Mar. 2012.
[7] Z. Gao and G. Guo, "Velocity free leader-follower formation control for autonomous underwater vehicles with line-of-sight range and angle constraints," *Inf. Sci.*, vol. 486, pp. 359–378, Jun. 2019.
[8] X. Dong, C. Sun, and G. Hu, "Time-varying output formation control for linear multi-agent systems with switching topologies," *Int. J. Robust Nonlinear Control*, vol. 26, no. 16, pp. 3558–3579, Nov. 2016.
[9] Z. Yan, Z. Yang, L. Yue, L. Wang, H. Jia, and J. Zhou, "Discrete-time coordinated control of leader-following multiple AUVs under switching topologies and communication delays," *Ocean Eng.*, vol. 172, pp. 361–372, Jan. 2019.
[10] Z.-X. Li and B.-L. Wang, "Robust attitude tracking control of spacecraft in the presence of disturbances," *J. Guid., Control, Dyn.*, vol. 30, no. 4, pp. 1156–1159, Jul. 2007.
[11] Y. Chang, Y. Wang, F. E. Alsaadi, and G. Zong, "Adaptive fuzzy output-feedback tracking control for switched stochastic pure-feedback nonlinear systems," *Int. J. Adapt. Control*, vol. 33, no. 10, pp. 1567–1582, 2019.
[12] Y. Chang, S. Zhang, N. D. Alotaibi, and A. F. Alkhateeb, "Observer-based adaptive finite-time tracking control for a class of switched nonlinear systems with unmodeled dynamics," *IEEE Access*, vol. 8, pp. 204782–204790, Sep. 2020.
[13] Y. Wang, N. Xu, Y. Liu, and X. Zhao, "Adaptive fault-tolerant control for switched nonlinear systems based on command filter technique," *Appl Math Comput*, vol. 392, pp. 1–18, Mar. 2021.
[14] T. Tang, Z. Liu, and Z. Chen, "Event-triggered formation control of multi-agent systems," in *Proc. Chin. Control Conf.*, Yantai, China, 2011, pp. 4783–4786.
[15] Z. Cai, H. Zhou, J. Zhao, K. Wu, and Y. Wang, "Formation control of multiple unmanned aerial vehicles by event-triggered distributed model predictive control," *IEEE Access*, vol. 6, pp. 55614–55627, Oct. 2018.
[16] J. Liu, Y. Yu, J. Sun, and C. Sun, "Distributed event-triggered fixed-time consensus for leader-follower multiagent systems with nonlinear dynamics and uncertain disturbances," *Int. J. Robust Nonlinear Control*, vol. 28, no. 11, pp. 3543–3559, Apr. 2018.

[17] Q. Yang, J. Li, and B. Wang, "Leader-following output consensus for high-order nonlinear multi-agent systems by distributed event-triggered strategy via sampled data information," *IEEE Access*, vol. 7, pp. 70799–70810, Jun. 2019.
[18] J. Cai, R. Yu, B. Wang, C. Mei, and L. Shen, "Decentralized event-triggered control for interconnected systems with unknown disturbances," *J. Franklin Inst.*, vol. 357, no. 3, pp. 1494–1515, Feb. 2020.
[19] A. Kamboj, N. K. Dhar, and N. K. Verma, "Event-triggered control for trajectory tracking by robotic manipulator," in *Computational Intelligence: Theories, Applications and Future Directions—Volume I* (Advances in Intelligent Systems and Computing), vol. 798. Singapore: Springer, Aug. 2018, pp. 161–170.
[20] D. Yue, E. Tian, and Q.-L. Han, "A delay system method for designing event-triggered controllers of networked control systems," *IEEE Trans. Autom. Control*, vol. 58, no. 2, pp. 475–481, Feb. 2013.
[21] G. Guo, L. Ding, and Q.-L. Han, "A distributed event-triggered transmission strategy for sampled-data consensus of multi-agent systems," *Automatica*, vol. 50, no. 5, pp. 1489–1496, May 2014.
[22] E. Garcia, Y. Cao, and D. W. Casbeer, "Decentralized event-triggered consensus with general linear dynamics," *Automatica*, vol. 50, no. 10, pp. 2633–2640, Oct. 2014.
[23] D. Yang, W. Ren, X. Liu, and W. Chen, "Decentralized event-triggered consensus for linear multi-agent systems under general directed graphs," *Automatica*, vol. 69, pp. 242–249, Jul. 2016.
[24] W. Hu, L. Liu, and G. Feng, "Output consensus of heterogeneous linear multi-agent systems by distributed event-triggered/self-triggered strategy," *IEEE Trans. Cybern.*, vol. 47, no. 8, pp. 1914–1924, Aug. 2017.
[25] S. Luo and D. Ye, "Double event-triggered control for linear multi-agent systems with augmented dynamic triggering mechanisms," *Appl. Math. Comput.*, vol. 386, pp. 1–14, Dec. 2020.
[26] C. Deng, W.-W. Che, and Z.-G. Wu, "A dynamic periodic event-triggered approach to consensus of heterogeneous linear multiagent systems with time-varying communication delays," *IEEE Trans. Cybern.*, early access, Sep. 29, 2020, doi: 10.1109/TCYB.2020.3015746.
[27] R. Wang, C. Si, H. Ma, and C. Hao, "Global event-triggered inner–outer loop stabilization of under-actuated surface vessels," *Ocean Eng.*, vol. 218, Dec. 2020, Art. no. 108228.
[28] Y. Ma, Z. Nie, Y. Yu, S. Hu, and Z. Peng, "Event-triggered fuzzy control of networked nonlinear underactuated unmanned surface vehicle," *Ocean Eng.*, vol. 213, Oct. 2020, Art. no. 107540.
[29] Y. Yang and D. Yue, "NNs-based event-triggered consensus control of a class of uncertain nonlinear multi-agent systems," *Asian J. Control*, vol. 21, no. 2, pp. 1–14, Mar. 2018.
[30] Z.-M. Li, X.-H. Chang, and J. H. Park, "Quantized static output feedback fuzzy tracking control for discrete-time nonlinear networked systems with asynchronous event-triggered constraints," *IEEE Trans. Syst., Man, Cybern. Syst.*, early access, Aug. 15, 2019, doi: 10.1109/TSMC.2019.2931530.
[31] X. You, C. Hua, and X. Guan, "Event-triggered leader-following consensus for nonlinear multiagent systems subject to actuator saturation using dynamic output feedback method," *IEEE Trans. Autom. Control*, vol. 63, no. 12, pp. 4391–4396, Dec. 2018.
[32] X. Chen and F. Hao, "Event-triggered average consensus control for discrete-time multi-agent systems," *IET Control Theory Appl.*, vol. 6, no. 16, pp. 2493–2498, Nov. 2012.
[33] J. Hu, G. Chen, and H. Li, "Distributed event-triggered tracking control of second-order leader-follower multi-agent systems," in *Proc. Chin. Control Conf.*, Yantai, China, 2011, pp. 4819–4824.
[34] Y. Li, G. Yang, and S. Tong, "Fuzzy adaptive distributed event-triggered consensus control of uncertain nonlinear multiagent systems," *IEEE Trans. Syst., Man, Cybern. Syst.*, vol. 49, no. 9, pp. 1777–1786, Sep. 2019.
[35] B. H. Wang, W. S. Chen, B. Zhang, and Y. Zhao, "Regulation cooperative control for heterogeneous uncertain chaotic systems with time delay: A synchronization errors estimation framework," *Automatica*, vol. 108, pp. 1–13, Oct. 2019.

AIHUA ZHANG received the Ph.D. degree from Harbin Engineering University, Harbin, China, in 2014. In 2014, she joined the Shanghai University of Engineering Science, as an Instructor. She is currently a Lecturer with the School of Mechanical and Automotive Engineering, Shanghai University of Engineering Science, Shanghai, China. She has authored or coauthored more than 20 peer-reviewed technical articles and a book. Her research interests include motion control of agents, distributed control systems, and event-triggered control techniques.

JIE ZHANG is currently pursuing the M.S. degree with the School of Mechanical and Automotive Engineering, Shanghai University of Engineering Science, Shanghai, China. Her current research interests include multi-USVs coordinated motion control and distributed control systems.

LINGYAO YANG is currently pursuing the M.S. degree with the School of Mechanical and Automotive Engineering, Shanghai University of Engineering Science, Shanghai, China. His current research interests include multi-agent coordinated motion control and distributed control systems.